Different outcomes for the *MYB* floral symmetry genes *DIVARICATA* and *RADIALIS* during the evolution of derived actinomorphy in *Plantago*

Wesley Reardon[1], Pauline Gallagher[1], Katie M. Nolan[1], Hayley Wright[1], Maria Cruz Cardeñosa-Rubio[2], Claudia Bragalini[3], Chui-Sang Lee[4], David A. Fitzpatrick[1], Killian Corcoran[1], Kirsten Wolff[5] and Jacqueline M. Nugent[1]

[1]Department of Biology, National University of Ireland Maynooth, Maynooth, Co. Kildare, Ireland; [2]Facultad de Biología, Universidad de Salamanca, Campus Miguel de Unamuno, 37007 Salamanca, Spain; [3]Department of Life Sciences and Systems Biology, University of Turin, Viale Mattioli 25, 10125 Turin, Italy; [4]School of Biotechnology, Dublin City University, Glasnevin, Dublin 9, Ireland; [5]School of Biology, Newcastle University, Ridley Building, Newcastle, NE1 7RU, UK

Summary

- The gene network that specifies flower shape in *Antirrhinum majus* (bilateral floral symmetry or zygomorphy) includes two *MYB*-class genes – *RADIALIS* (*RAD*) and *DIVARICATA* (*DIV*). *RAD* is involved in establishing the dorsal identity program and its role is to regulate the domain of activity of *DIV* (the ventral identity program) by restricting it to ventral regions of the flower.
- *Plantago* is in the same family as *Antirrhinum* but has small, radially symmetrical (actinomorphic) flowers derived from a zygomorphic ancestral state. Here we investigate the *MYB*-class floral symmetry genes and the role they have played in the evolution of derived actinomorphy in *Plantago lanceolata*.
- A *DIV* ortholog (*PlDIV*) but no *RAD* ortholog was identified in *P. lanceolata*. *PlDIV* is expressed across all petals and stamens later in flower development, which is consistent with the loss of *RAD* gene function. *PlDIV* expression in anther sporogenous tissue also suggests that *PlDIV* was co-opted to regulate cell proliferation during the early stages of pollen development.
- These results indicate that evolution of derived actinomorphy in *Plantago* involved complete loss of dorsal gene function, resulting in expansion of the domain of expression of the ventral class of floral symmetry genes.

Introduction

The floral symmetry gene network is best understood in the model plant *Antirrhinum majus*, where bilateral symmetry (zygomorphy) is exhibited in the distinct shape of dorsal, lateral and ventral petals and by dorsal stamen abortion (Coen, 1996; Luo *et al.*, 1996). *CYCLOIDEA* (*CYC*) and *DICHOTOMA* (*DICH*) are key genes that determine the shape of dorsal floral organs (in particular the petals) in *Antirrhinum* (Luo *et al.*, 1996, 1999; Almeida *et al.*, 1997; Galego & Almeida, 2002). *CYC* and *DICH* are paralogous ECE-CYC2-class genes of the TCP (*TEOSINTE BRANCHED 1* (*TB1*), *CYCLOIDEA* (*CYC*) and *PROLIFERATING CELL NUCLEAR ANTIGEN FACTOR* (*PCF*)) transcription factor family and are thought to have a role in regulating cell proliferation and expansion (Cubas *et al.*, 1999a; Howarth & Donoghue, 2006; Martin-Trillo & Cubas, 2009). In *Antirrhinum*, both *CYC* and *DICH* (*CYC2* genes) are expressed in the dorsal region of very early flower meristems and expression of both genes is maintained throughout

flower development in dorsal floral organs (Luo *et al.*, 1999). In *cyc/dich* double mutants, *Antirrhinum* flowers lose their distinct bilateral symmetry and become radially symmetrical (actinomorphic) and all petals and stamens resemble the ventral petals and stamens of wild-type flowers (Luo *et al.*, 1999; Corley *et al.*, 2005). Two additional genes, *DIVARICATA* (*DIV*) and *RADIALIS* (*RAD*), act with the *CYC2* genes to specify flower shape in *Antirrhinum*. Both DIV and RAD proteins belong to the MYB protein superfamily (Galego & Almeida, 2002; Corley *et al.*, 2005). *CYC2* genes positively regulate *RAD* expression in the dorsal regions of the flower and *rad* mutant flowers resemble *cyc/dich* mutant flowers in their phenotype (Corley *et al.*, 2005). *DIV* is required to specify organ shape in ventral regions of the flower and in *div* mutant flowers the ventral petals adopt lateral petal shape (Almeida *et al.*, 1997; Galego & Almeida, 2002). *DIV* is transcribed throughout the floral meristem; however, *DIV* activity is repressed in dorsal regions, that is, where the domains *DIV*, *CYC2* and *RAD* gene expression overlap, by RAD binding to a co-regulator of DIV transcriptional activity called DIV- and

RAD-interacting factor (DRIF) and sequestering it in the cytoplasm (Raimundo *et al.*, 2013). When dorsal and ventral identity programs are eliminated in a *cyc/dich/div* triple mutant, the default lateral floral organ identity program is revealed in *A. majus* (Almeida *et al.*, 1997; Corley *et al.*, 2005).

Actinomorphy is considered the ancestral floral shape condition in flowering plants (Doyle & Endress, 2000; Endress & Doyle, 2009). However, phylogeny mapping suggests that zygomorphy has evolved independently at least 70 times during angiosperm evolution: once in basal angiosperms, at least 23 times independently in monocots and at least 46 times independently in eudicots (Citerne *et al.*, 2010). In particular, zygomorphy is more prevalent within some of the more recently derived, species-diverse lineages of flowering plants (Ronse De Craene *et al.*, 2003; Sargent, 2004). A surprising aspect of zygomorphy is that, although it evolved independently many times, on several occasions it did so by co-opting the same *CYC2*-class genes into the floral symmetry gene network. *Arabidopsis thaliana* produces radially symmetric flowers and, although an *A. thaliana CYC2* gene is expressed in dorsal regions of the early flower meristems, expression is not maintained during later stages of flower development (Cubas *et al.*, 2001). Maintenance of *CYC2* gene expression in dorsal floral organs throughout flower development correlates very strongly with zygomorphy in a range of diverse angiosperms including Lamiales, Fabales, Brassicales, Asterales, and Malpighiales (Hileman *et al.*, 2003; Feng *et al.*, 2006; Busch & Zachgo, 2007; Broholm *et al.*, 2008; Kim *et al.*, 2008; Wang *et al.*, 2008; Zhou *et al.*, 2008; Zhang *et al.*, 2010; Chapman *et al.*, 2012). *CYC2* genes, therefore, are a conserved feature of floral symmetry gene networks across diverse plant taxa as a result of parallel evolutionary processes.

Molecular phylogenetics places *Plantago* and *Antirrhinum* within a highly supported clade within the Lamiales, *sensu lato* called the Veronicaceae (Olmstead *et al.*, 2001) or the Plantaginaceae (Rønsted *et al.*, 2002). Despite their relatively close phylogenetic relatedness, these genera produce strikingly different flowers and have adopted very different reproductive strategies (Reeves & Olmstead, 1998; Reardon *et al.*, 2009). In contrast to the large zygomorphic, insect-pollinated flowers of *Antirrhinum*, *Plantago* flowers are small and actinomorphic and are wind-pollinated (Reardon *et al.*, 2009). *Plantago* species are also gynodioecious, that is, both female and hermaphrodite plants coexist within a population: females are effectively male-sterile, whereas hermaphrodites have functional female and male reproductive organs (van Damme & van Delden, 1982; De Haan *et al.*, 1997). The genetics of sex determination in plants involves both nuclear and cytoplasmic gene interactions – mitochondrial genes cause male sterility (female flowers) and nuclear genes restore male fertility (hermaphrodite flowers) (Delph *et al.*, 2006). Thus, mitochondrial-to-nuclear retrograde signaling has a profound influence on flower morphology (Carlsson *et al.*, 2008). Two female types (male sterile 1 (MS1) and male sterile 2 (MS2)) have been described for *Plantago lanceolata* (van Damme & van Delden, 1982; De Haan *et al.*, 1997).

Derived actinomorphy in a range of flowering plant genera including *Cadia* (Citerne *et al.*, 2006), *Bournea* (Zhou *et al.*, 2008), *Linaria* (Cubas *et al.*, 1999b) and several genera within the Malpighiaceae (Zhang *et al.*, 2013) has been shown to correlate with changes in the domain of expression of *CYC2* genes. Gene loss events have also been implicated as facilitators of flower shape change. Preston *et al.* (2011) have proposed that derived actinomorphy in *Plantago* is the result of loss of the entire floral symmetry gene network (*CYC2*, *DIV* and *RAD*). They showed that a *CYC2* gene loss event (A-clade *CYC*) correlates with derived actinomorphy in *Plantago* and is associated with expansion of the domain of expression, and possible neofunctionalization, of a second *CYC2* gene in *Plantago major* (B-clade *PmCYC*). In a previous study we reported a single *CYC2* gene in *P. lanceolata* (B-clade *PlCYC*) that has no dorsal-specific expression during flower development and has a much more restricted domain of expression compared with *PmCYC* (Reardon *et al.*, 2009). The two studies are consistent with loss of A-clade *CYC* correlating with the evolution of derived actinomorphy in *Plantago* but suggest that B-clade *CYC* gene regulation followed different trajectories in different *Plantago* lineages: some losing B-clade *CYC* expression during early stages of flower development (*PlCYC*; Reardon *et al.*, 2009) and others maintaining a broad pattern of B-clade *CYC* expression during flower development (*PmCYC*; Preston *et al.*, 2011). The aim of this study was to investigate the fate of the MYB-class floral symmetry genes *DIV* and *RAD* and the role they may have played in the evolution of derived actinomorphy in *P. lanceolata*.

Materials and Methods

Plant material

Fresh *P. lanceolata* L. and *P. major* L. leaf and inflorescence tissue used for gene cloning experiments was obtained from plants growing wild at the National University of Ireland, Maynooth, Ireland. *In situ* hybridization was carried out on inflorescence tissue obtained from *P. lanceolata* plants growing wild at the University of Edinburgh, Scotland and on inflorescence tissue obtained from segregating hermaphrodite and MS1 (female) plants generated by crossing an MS1 maternal parent with a hermaphrodite paternal parent (Cross B: NPZH 22-9 X FREQ 1-13; results in a 1 : 1 segregating population of hermaphrodite and MS1 plants). Fresh *Digitalis purpurea* and *Veronica longifolia* leaf tissue was obtained from plants grown from seed obtained from Kings Wholesale Seed Merchants and Growers, Essex, UK. Fresh *Streptocarpus prolixus* leaf tissue was obtained from plants growing in the National Botanic Gardens, Glasnevin, Dublin.

DIV and *RAD* gene isolation

Plantago lanceolata DIV-like PCR products were generated using MYB1F and DIV1R primers (Supporting Information Table S1) using inflorescence cDNA isolated from total RNA as a template. PCR cycling conditions were 94°C for 1 min; 40 cycles of 94°C for 45 s, 45°C for 90 s, and 72°C for 3 min; a

final extension at 72°C for 10 min and a 4°C hold. *Plantago major DIV*-like PCR products were generated using PlDIVqPCRF and DIV1R primers (Table S1) using genomic DNA isolated from leaf tissue as the template DNA. PCR cycling conditions were 95°C for 1 min; 35 cycles of 95°C for 45 s, 50°C for 30 s, and 72°C for 45 s; followed by a final extension at 72°C for 10 min and a 4°C hold. PCR products were cloned into either the pCR2.1 or pCR4 TOPO cloning vector and sequenced. DNA sequences were assessed for similarity to *A. majus DIV* by BLAST analysis. Sequence alignments were generated using the profile alignment option in CLUSTALX (Thompson *et al.*, 2002; GenBank references, Table S2). The final alignments were manually inspected to ensure no ambiguities existed. The optimum model of molecular evolution (HKY+G) was determined using MODELGENERATOR v0.85 (Keane *et al.*, 2006). One hundred bootstrap replicates were carried out with the appropriate model of evolution using the software program PHYML (Guindon & Gascuel, 2003) and summarized using the majority-rule consensus method. Alternative tree topologies were assessed using the approximately unbiased test for statistical differences in alternative phylogenetic trees implemented in the software package CONSEL (Shimodaira, 2002). A PCR strategy was also used to amplify *RAD* gene orthologs from *P. lanceolata*; *D. pupurea*, *V. longifolia*, and *S. prolixus* template DNAs were used as positive controls. Initially PCR was carried out using various combinations of forward and reverse *RAD* gene-specific primers (Table S1) and using genomic DNA isolated from leaf tissue as the template DNA. All PCR reactions were repeated using *P. lanceolata* inflorescence cDNA as the template. The *RAD*-like gene family was more broadly assessed in *P. lanceolata* using the primer combinations designed by Boyden *et al.* (2012) (GB-RAD primers; Table S1). PCR products were cloned into the pCR4 TOPO cloning vector and 34 confirmed recombinants, with inserts of the expected size, were sequenced. The sequences were cropped to remove all primer sequences. Nucleotide and amino acid alignments were performed manually using only the unique sequences. A nucleotide alignment was used to construct a phylogeny in PAUP using the maximum likelihood (ML) method with the Generalised time-reversible (GTR) model of sequence evolution (GenBank references, Table S3). One hundred bootstrap replicates were also performed.

Quantitative RT-PCR

Total RNA was extracted from mature stamens (late-stage flowers: petals were enlarged and folded back, and stamens were exserted) and whole inflorescences from *P. lanceolata* hermaphrodite and MS1 plants using an RNeasy Plant Mini Kit (Qiagen). cDNA synthesis was carried out using 1 μg of total RNA using a Transcriptor High Fidelity cDNA Synthesis Kit (Roche). Tissue-specific qRT-PCR analyses were performed using the SYBR-Green methodology and gene-specific primers (Table S1). Three biological replicates (including three technical replicates for each) were included for each tissue type. The levels of *PlCYC* and *PlDIV* transcripts were normalized to the level of a

CALMODULIN (*CAM*) control. *CAM* was chosen as the control gene after preliminary qRT-PCR experiments showed that the *CAM* primers gave very consistent cycle threshold (Ct) means when used across a dilution series of petal, stamen and inflorescence cDNAs. Relative gene expression levels were graphed using the iQ5 OPTICAL SYSTEM SOFTWARE version 1.0 (Bio-Rad). All classes of qPCR products were cloned and sequenced to confirm the identity of the amplified gene products. *PlCAM* has GenBank accession number KF964144.

In situ hybridization and toluidine blue staining

RNA *in situ* hybridization was carried out as described previously (Reardon *et al.*, 2009). *PlDIV*, *PlCYC* and *P. lanceolata HISTONE4* (*PlH4*, a marker for cells in the DNA replication phase of mitosis) gene-specific regions were cloned into the pCR®II-TOPO® vector (Invitrogen). *PlH4* has GenBank accession number KF964141. Antisense and sense DIG-labeled riboprobes were generated by transcription from the SP6 and T7 promoters using a DIG RNA Labeling Kit (SP6/T7; Roche). Wax-embedded inflorescence tissue from hermaphrodite and MS1 plants (similar to that used for *in situ* hybridization experiments) was sectioned (7-μM sections) and stained with 1% toluidine blue for 5 min before the sections were washed in dH$_2$0.

Results

DIV- and *RAD*-like genes in *Plantago*

Initially, two *P. lanceolata DIV*-like sequences were cloned and sequenced using PCR and primers specific to regions of the conserved MYBI and MYBII domains of *DIV* (Galego & Almeida, 2002). Phylogenetic analyses of these and related sequences in the databases showed one of these *DIV*-like sequences nested within a well-supported clade that includes the *Antirrhinum DIV* and *DIV*-like genes, suggesting that this sequence is from a *P. lanceolata DIV* ortholog (*PlDIV*; Fig. 1a). A *P. major DIV* ortholog was also identified using PCR and primers based on the *PlDIV* sequence (*PmDIV*; Fig. 1a). Broadly speaking, the inferred gene relationships within the *DIV* clade (Fig. 1a) are consistent with known species relationships. The main exception is the inferred sister relationship between *Plantago/Aragoa* and *Digitalis*, which has relatively low bootstrap support (Fig. 1a). Other more extensive gene phylogenies support a relationship between *Plantago/Aragoa* and *Wulfenia/Veronica* with *Digitalis* the outgroup to these genera (Preston *et al.*, 2011). However, there is no statistical difference ($P < 0.05$) between the log likelihood value of this tree (−4769.80, Fig. 1a) and that of an alternative tree with *Plantago/Aragoa* and *Wulfenia/Veronica* as sister groups to the exclusion of *Digitalis* (−4771.30); thus, either tree topology is equally likely. The second *P. lanceolata DIV*-like sequence identified in this study (*PlDIV2*; Fig. 1a) is similar to other more distantly related *DIV* paralogs previously identified in *Plantago coronopus* and *P. lanceolata* (Preston *et al.*, 2011).
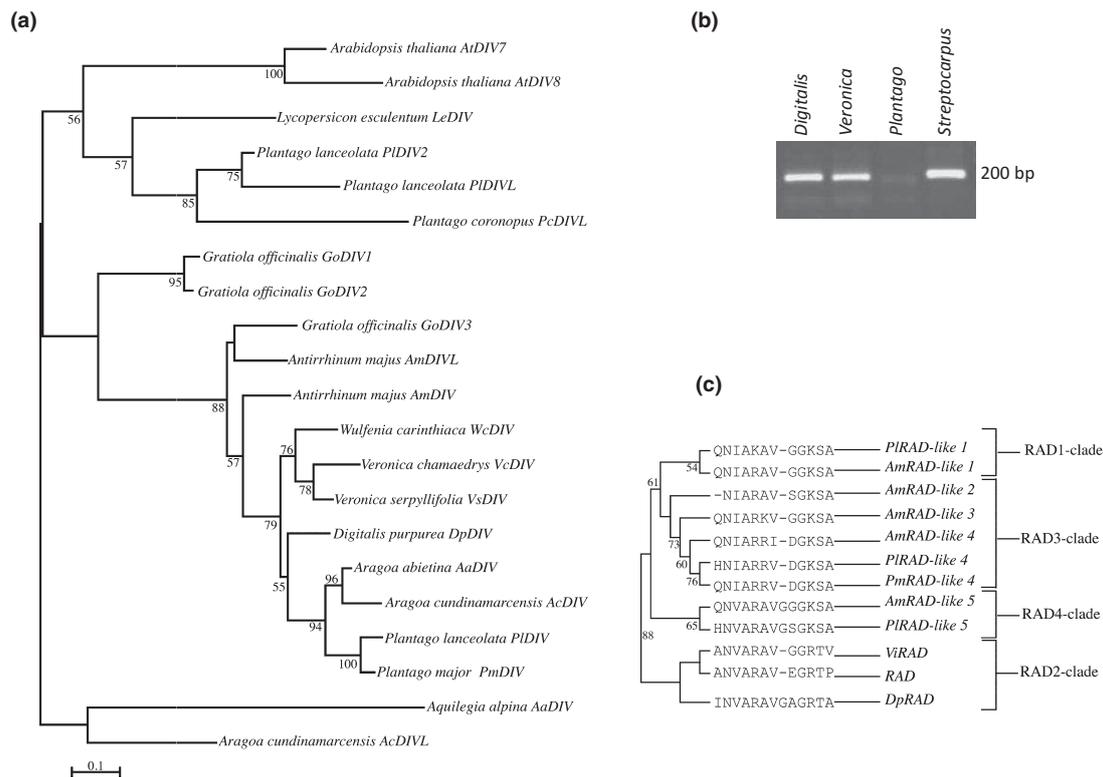
Fig. 1 *DIVARICATA* (*DIV*)-like and *RADIALIS* (*RAD*)-like genes in *Plantago lanceolata* and related species. (a) Maximum likelihood (ML) tree showing the relationships between representative *DIV*-like loci. Bootstrap values are displayed at selected branches. (b) PCR amplification of a *RAD* gene region in *Digitalis purpurea*, *Veronica longifolia* and *Streptocarpus prolixus* but not in *P. lanceolata*. (c) ML tree showing the relationships between *RAD*-like loci in *Plantago* and *Antirrhinum majus* (*Veronica intercedens* (*Vi*) and *Digitalis pupurea* (*Dp*) sequences are also included in the RAD2 clade). Bootstrap values are displayed at selected branches. The deduced amino acid sequence for each nucleotide sequence is shown at the relevant branch tip.

Several primer combinations and a range of PCR conditions were used to try to amplify a *RAD* gene ortholog from *P. lanceolata*. All attempts to generate a convincing PCR product failed, this despite the fact that PCR products of the expected size were easily obtained from two other Veronicaceae species (*D. purpurea* and *V. longifolia*) and one non-Veronicaceae species (*S. prolixus*; Fig. 1b). The same primer combinations and range of PCR conditions also failed to generate a PCR product from *P. lanceolata* inflorescence cDNA. These data suggested the absence of a *RAD* gene ortholog in *P. lanceolata*. A more comprehensive investigation of *RAD*-like genes in *P. lanceolata* was carried out, using more universal, gene-family-specific PCR primers designed by Boyden *et al.* (2012). Three classes of *P. lanceolata RAD*-like sequences were identified using this approach (Fig. 1c): (1) sequences that fall within the RAD1-clade of *RAD*-like genes identified by Boyden *et al.* (2012); (2) sequences that fall within the RAD3-clade of *RAD*-like genes identified by Boyden *et al.* (2012); (3) sequences that are most similar to *A. majus RAD-like5* (Baxter *et al.*, 2007; Fig. 1c; designated as a RAD4 clade). None of the *P. lanceolata* sequences fall within the RAD2 clade that includes *A. majus RAD* and other *RAD* gene orthologs (Fig. 1c; Boyden *et al.*, 2012). This despite the fact that, in the Dipsacales, the same PCR primers selectively

amplified more RAD2-clade sequences than any other *RAD*-like sequences (Boyden *et al.*, 2012). These data strongly support the conclusion that *P. lanceolata* does not have a *RAD* gene ortholog and confirm previous work that reported the absence of this gene in a range of *Plantago* species (Preston *et al.*, 2011).

PlDIV is expressed in all petals and stamens during late-stage flower development in *P. lanceolata*

RNA *in situ* hybridization was carried out to establish the spatial and temporal pattern of expression of *PlDIV* during flower development in *P. lanceolata* (Fig. 2a). The early pattern of *PlDIV* expression was very similar to that reported for *DIV* in *A. majus* (*AmDIV*; Galego & Almeida, 2002). A low level of *PlDIV* expression was seen in the apical inflorescence meristem (Fig. 2b); *PlDIV* was expressed throughout early floral meristems before the initiation of floral organs and was transiently expressed in the bract primordia that subtend floral meristems (Fig. 2b,c); *PlDIV* was expressed in all early developing floral organs (Fig. 2d) before being down-regulated in sepals (Fig. 2e). However, the later pattern of *PlDIV* expression differed from that reported for *AmDIV*. *PlDIV* was initially expressed across all tissues of all four petals (Fig. 2e); as petal development
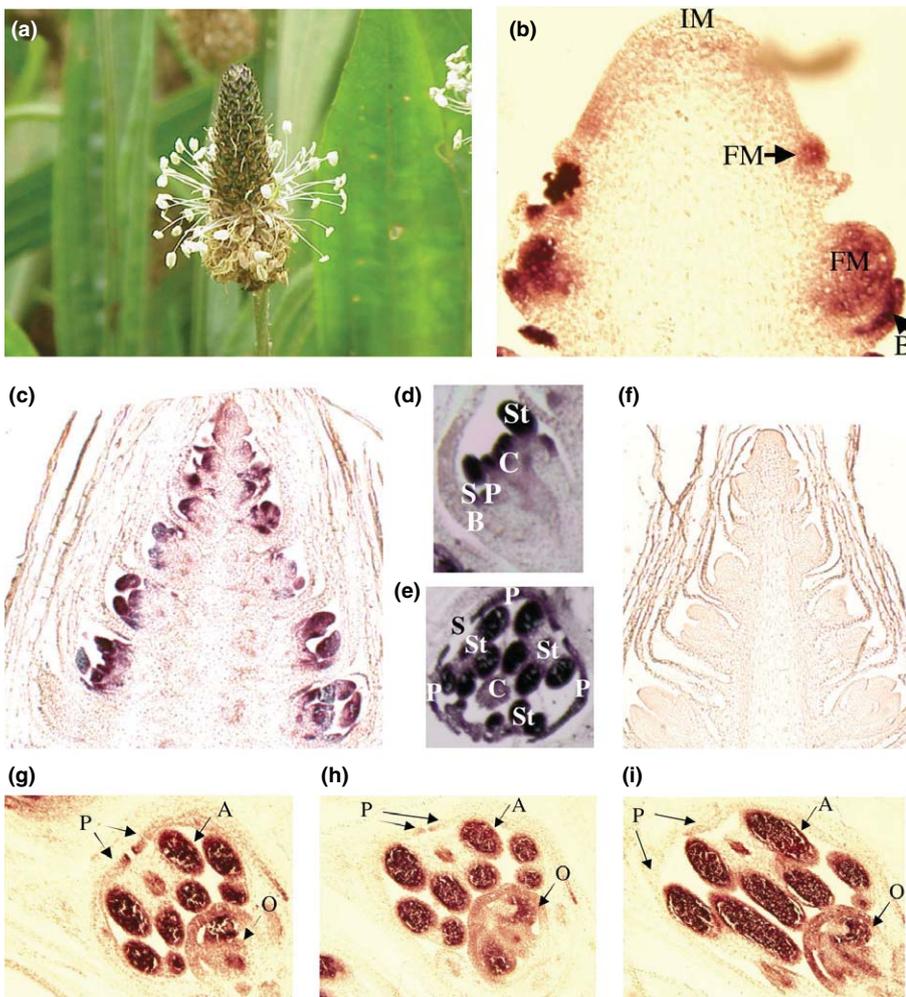
Fig. 2 *Plantago lanceolata DIVARICATA* (*PlDIV*) is expressed in the inflorescence meristem and in all lateral organs. (a) Hermaphrodite *P. lanceolata* inflorescence – the flowers are protogynous; young flowers with exserted stigmas are located toward the top of the inflorescence, and older flowers with exserted stamens are located toward the bottom of the inflorescence. (b) Longitudinal section through the main inflorescence apex hybridized with a *PlDIV* antisense probe. *PlDIV* is expressed in the inflorescence meristem (IM), throughout early flower meristems (FM) and transiently in bract primordia (B). (c–e) *PlDIV* is expressed in all developing floral organs (S, sepals; P, petals; St, stamens; C, carpels), before being down-regulated in the sepals (e). (f) Similar stage tissue sections probed with the *PlDIV* sense control probe. (g–i) Later in flower development *PlDIV* expression ceases in petals, although expression is maintained for longer at lateral petal edges (P). A high level of *PlDIV* expression is maintained in the anthers of developing stamens (A), and a low level of expression is also maintained throughout ovule development within the carpel (O).

proceeded, expression became restricted to the lateral edges of petals (Fig. 2g) until eventually expression ceased completely in these floral organs (Fig. 2h,i). The most distinguishing aspect of later *PlDIV* expression was the extremely high level of mRNA accumulation seen in anther tissue throughout stamen development; a low level of *PlDIV* expression was also maintained within the ovary of the carpel (Fig 2g–i). No hybridization signal was detected in tissue sections probed with the same amount of *PlDIV* sense control probe (Fig. 2f).

In order to understand the role *PlDIV* might play in anther tissue, gene expression was assessed more closely at different stages of anther and pollen development. First, anther and early pollen development was examined in *P. lanceolata* by staining semi-thin tissue sections with toluidine blue. A developmental series showing representative pre-meiotic, meiotic and post-meiotic anther developmental stages is presented in Fig. 3 (a–f). Stage-matched anther sections probed with *PlDIV* are shown in Fig. 3 (g–l). *PlDIV* was highly expressed in the microspore mother cells during pre-meiotic stages of anther development (Fig. 3g,h). *PlDIV* expression decreased and eventually ceased in the microspore mother cells during meiosis but expression was maintained in the tapetal cell layer (Fig. 3i,j). A high level of *PlDIV* expression was maintained within the tapetal cells up until the time at which

tetrads were formed (Fig. 3k), after which expression decreased in tapetal cells and ceased completely by the time the haploid microspores were released (Fig. 3l). This pattern of expression suggests that *PlDIV* is specifically expressed in cells that are proliferating and undergoing mitosis during anther development. This was confirmed by carrying out *in situ* hybridization using *PlH4* as a marker for cell division. The congruence between the pattern of *PlDIV* and *PlH4* expression during anther development is striking. Like *PlDIV*, *PlH4* was expressed in the sporogenic tissue until the microspore mother cells entered meiosis and in the tapetum cells up until the tetrad stage (Fig. 3m–q). These data suggest that both *AmDIV* and *PlDIV* have a conserved role in regulating cell proliferation – albeit cell proliferation in petals in *Antirrhinum* (Galego & Almeida, 2002) and in stamens in *P. lanceolata*.

Premature down-regulation of *PlDIV* expression in MS1 (female) flowers

As the expression data suggested that *PlDIV* may have a role in regulating cell proliferation during stamen development, we examined *PlDIV* expression in *P. lanceolata* MS1 plants.
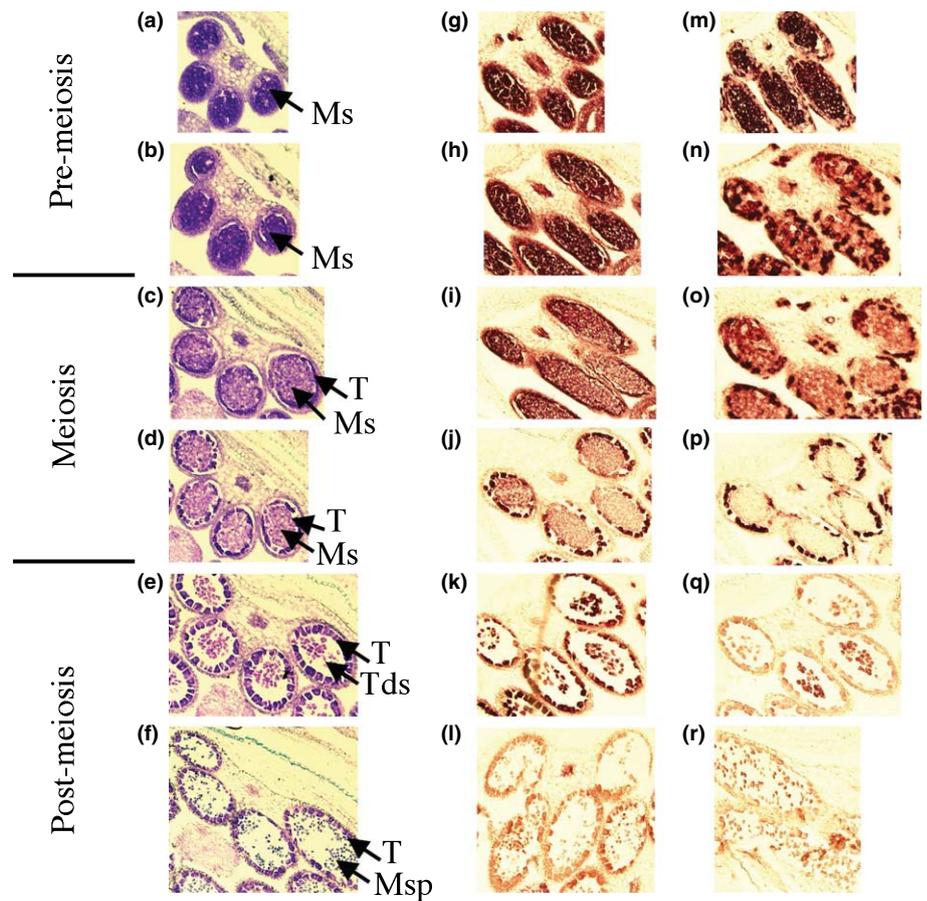
Fig. 3 *Plantago lanceolata DIVARICATA* (*PlDIV*) is expressed during the early stages of pollen development in hermaphrodite flowers. (a–f) *P. lanceolata* anther sections stained with 1% toluidine blue showing representative pre-meiotic (a, b), meiotic (c, d) and post-meiotic (e, f) stages of pollen development. *PlDIV* is expressed in primary sporogenous tissue and in the tapetum and microspore mother cells within developing locules (g, h). Expression ceases in the microspore mother cells during meiosis (i, j). Expression is maintained within the tapetal cells until tetrads are formed (k) and ceases by the time the haploid microspores are released (l). The pattern of *PlH4* expression closely resembles that of *PlDIV* (m–r). Ms, microspore mother cells; T, tapetum; Tds, tetrads; Msp, microspores.

Flower development is normal in MS1 plants except that stamen filaments are shorter than in hermaphrodites and the anthers do not produce pollen (Fig. 4a–c; van Damme & van Delden, 1982). Real-time qPCR analysis showed no significant difference in the level of transcription of *PlDIV* in mature stamens of hermaphrodite and MS1 plants. However, *PlDIV* expression levels were on average 50% reduced in MS1 inflorescences compared with hermaphrodites (Fig. 4d). *PlCYC* transcript levels were also assessed as an internal control and were similar in the two inflorescence types (Fig. 4d). Because *PlDIV* expression levels appeared reduced in MS1 inflorescences, *in situ* hybridization was carried out to see how this might be reflected in the tissue-specific pattern of expression of the gene. The pattern of *PlDIV* expression in MS1 inflorescence tissue was similar to that seen in hermaphrodites up to the point when microspore mother cells entered meiosis (Fig. 5a, b). After the commencement of meiosis in MS1 anthers, *PlDIV* expression decreased significantly in the sporogenic tissue and also in the tapetal cells (Fig. 5c,d). Normal pollen development does not proceed beyond this point in MS1 anthers: anther locules became more flaccid than in hermaphrodites, the sporogenous tissue within the locules begins to disintegrate and tetrads and microspores are not produced (Fig. 5e). Again, the pattern of *PlH4* expression mirrored that of *PlDIV* in MS1 anthers; *PlH4* was expressed in the sporogenic tissue and in the tapetal cells until the microspore mother cells entered meiosis (Fig. 5f,g) after which point *PlH4* expression ceased in both these tissues (Fig. 5h,i). These data demonstrate premature down-regulation of *PlDIV* expression in tapetal cells in *P. lanceolata* MS1 flowers and that this down-regulation correlates with the failure of microspore mother cells to complete meiosis. In *P. lanceolata* MS1 flowers, *PlCYC* was expressed in anther connective tissue in a pattern similar to that reported previously for *P. lanceolata* (Fig. 5j–l; Reardon *et al.*, 2009).

Discussion

This study shows that *Plantago* retains just one of the MYB genes (*DIV*) that make up the flower shape gene regulatory network found in *A. majus*. *AmDIV* has a role in regulating cell division in the ventral petals and adjacent regions of lateral petals, giving these petals their distinctive shape (Galego & Almeida, 2002; Corley *et al.*, 2005). While the early pattern of *PlDIV* expression in *P. lanceolata* is similar to that reported for *AmDIV* (Galego & Almeida, 2002), the two genes differ in their later pattern of expression. Later *PlDIV* expression in hermaphrodite and MS1 flowers suggests that *PlDIV* has been redeployed to regulate cell proliferation during stamen development rather than petal development in *P. lanceolata*. Although the MYB floral symmetry genes, *RAD* and *DIV*, have not been studied as extensively as the *CYC2* genes in species other than *A. majus*, their role appears to
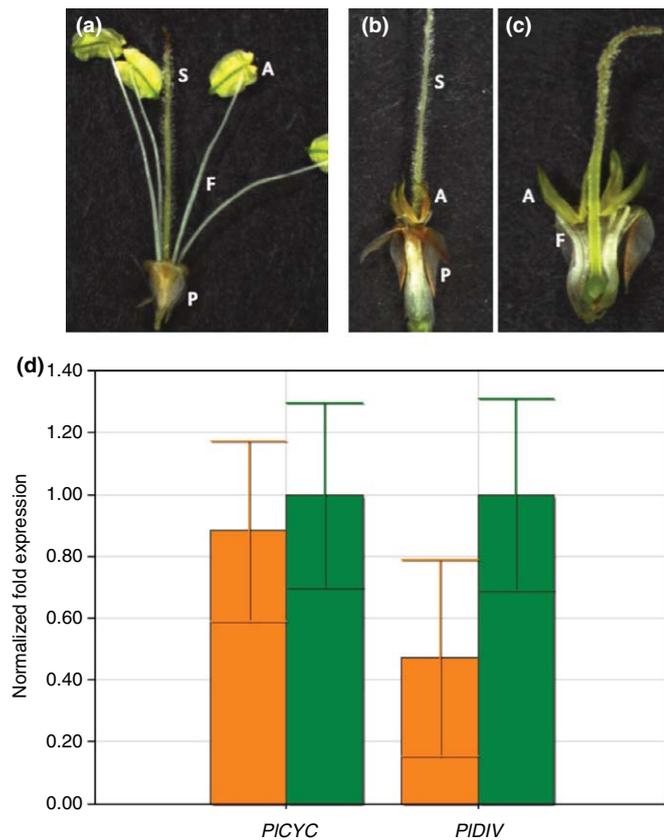
Fig. 4 *Plantago lanceolata DIVARICATA* (*PlDIV*) is prematurely down-regulated during the early stages of pollen development in male sterile 1 (MS1) flowers. (a) Mature *Plantago lanceolata* hermaphrodite flower – the petals are folded back and the mature stamens are exserted. (b, c) Mature *P. lanceolata* MS1 flowers: (b, c): the bracts and sepals have been removed; (c) a petal has been removed to reveal the short MS1 stamen filaments. S, stigma; A, anther; F, filament; P, petal. (d) Quantitative RT-PCR analyses showing relative *PlCYC* and *PlDIV* expression in *P. lanceolata* hermaphrodite (green) and MS1 (orange) inflorescence tissue. Error bars indicate ± 1 SD.

be conserved at least across the Lamiales (Zhou *et al.*, 2008). For example, *Bournea leiophyll* flowers have a single plane of symmetry (zygomorphy) during early floral organ initiation but transition to polysymmetry (actinomorphy) by the time the floral organs are mature. This switch from bilateral to radial symmetry at anthesis is achieved by the down-regulation of *BlRAD* in dorsal floral regions later in flower development and is associated with expression of *BlDIV* across all petals and stamens (Zhou *et al.*, 2008). The later pattern of *PlDIV* expression shares similarities with the expression pattern reported for *BlDIV*. In *B. leiophyll*, *BlDIV* is expressed later in flower development at the lateral edges of all petals and in all stamens before expression is down-regulated in both organ types (Zhou *et al.*, 2008). *B. leiophyll* flowers have five near-equal size stamens and it has been suggested that *BlDIV* expression in all stamen primordia may be involved in synchronizing stamen growth (Zhou *et al.*, 2008). *Plantago lanceolata* has four stamens of equal size (Fig. 4a) and continuous expression of *PlDIV* in all stamen primordia may also be synchronizing growth in these organs. Uniquely in

P. lanceolata, though, a very high level of *PlDIV* expression is maintained within stamen sporogenic cells until the stage when microspore mother cells enter meiosis and in tapetal cells until the microspores are released; this is not seen for either the *AmDIV* or *BlDIV* genes. The pattern of *PlH4* expression very closely mirrors that of *PlDIV* (Fig. 3g–r). In several plant species, cytoplasmic male sterility (CMS) is associated with tapetal programmed cell death (PCD) occurring earlier in anther development than in wild type (Horner & Rogers, 1974; Bino, 1985; Grant *et al.*, 1986; Balk & Leaver, 2001; Wilson *et al.*, 2001; Kapoor *et al.*, 2002; Ku *et al.*, 2003). Tapetal PCD normally occurs late in pollen development and is required to provide the precursors for the biosynthesis of the pollen outer wall (Parish & Li, 2010). It has been proposed that cell proliferative and degenerative forces act simultaneously during tapetum development and when the gene, or genes, required for cell proliferation are down-regulated, the degenerative cell death mechanism proceeds unchecked, causing tapetum degeneration (Kapoor *et al.*, 2002). Vacuolation and enlargement of tapetal cells commence at microspore mother cell meiosis in many plant species (Parish & Li, 2010). In hermaphrodite *P. lanceolata*, the tapetal cells also become enlarged and very clearly distinct at this stage (Fig. 3c,d). However, no distinct tapetal cell layer is seen in MS1 plants and this correlates with a premature down-regulation of *PlDIV* expression in tapetal cells (Fig. 5c,d). Although the tapetal layer is not as obvious in MS1 plants as it is in the hermaphrodites, it is clear that a tapetal cell layer is initiated, as evidenced by the pattern of *PlH4* expression (Fig. 5g). Eventually *PlDIV* and *PlH4* expression ceases in all cells within the MS1 anthers (Fig. 5e). At this stage it is not possible to say if cessation of *PlDIV* and *PlH4* expression in MS1 tapetum cells is attributable to gene-specific down-regulation in these cells and/or PCD. The cytology in the MS1 probed sections suggests tapetal cell shrinkage, which is an indicator of PCD (Parish & Li, 2010). It is possible then that the *P. lanceolata* MS1 phenotype is a result of premature tapetal PCD brought about by the loss of a counter-balancing *PlDIV*-mediated cell proliferative force. However, rather than initiating a tapetum cell death program, the down-regulation of *PlDIV* expression in MS1 anthers could equally well be a consequence of the cell death program itself, initiated by entirely different factors. Additional work is required to investigate the precise role of *PlDIV* in tapetum and pollen development.

All efforts to identify a *P. lanceolata RAD* ortholog failed, suggesting that this gene is absent in *P. lanceolata*. Several lines of evidence strongly support this conclusion: (1) *RAD* orthologs were easily identified in other Veronicaceae species (e.g. *V. longifolia* and *D. purpurea*) and in *S. prolixus*, a non-Veronicaceae species that also belongs to the Lamiales *sensu lato*, suggesting that the gene-specific primers and PCR methodologies used were appropriate for gene amplification; (2) several other *P. lanceolata* genes were easily identified using PCR in this study (including *PlCYC*, *PlCAL*, *PlDIV*, *PlDIV2* and *PlH4*), suggesting that an accelerated nucleotide substitution rate in *P. lanceolata* nuclear DNA cannot explain the lack of a *RAD* gene PCR product; (3) analysis of the extended *RAD*-like gene family in *P. lanceolata* also revealed no *RAD* gene ortholog even though all other known

Fig. 5 *Plantago lanceolata DIVARICATA* (*PlDIV*) expression is prematurely down-regulated in *Plantago lanceolata* male sterile 1 (MS1) anthers. (a–e) Expression pattern of *PlDIV* in MS1 anthers. Developmentally matched sections are shown for two different inflorescences (a1–e1 and a2–e2). After the commencement of meiosis, *PlDIV* expression decreases in the sporogenic tissue and in the tapetal cells (c, d) and normal pollen development does not proceed beyond this point (e). (f–i) Expression pattern of *PlH4* in MS1 anthers: *PlH4* is expressed in the sporogenic tissue and in the tapetal cells until the microspore mother cells enter meiosis (f–g), then *PlH4* expression ceases in both tissues (h–i). *PlCYC* is expressed in MS1 anther connective tissue (j–l). Ms, microspore mother cells; T, tapetum; CT, connective tissue.
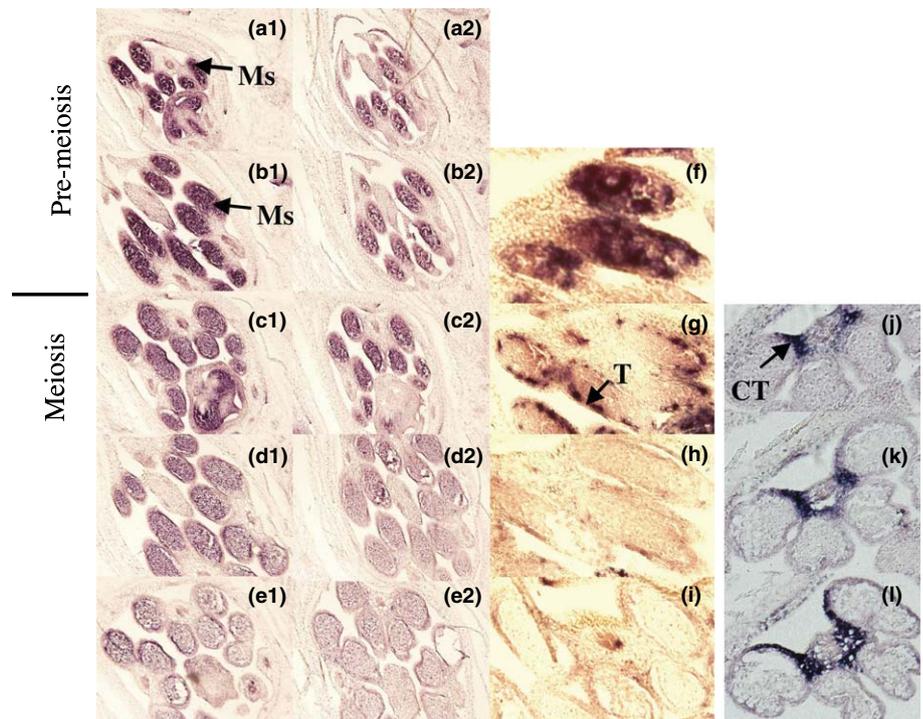
classes of *RAD*-like genes were identified using this approach, and despite the fact that the same PCR primers selectively amplified *RAD* gene orthologs from a range of species within the Dipsacales (Boyden *et al.*, 2012); (4) late *PlDIV* expression seen in all *P. lanceolata* petals is consistent with a *RAD* gene loss event. These data also confirm previous work that showed *RAD* gene loss in the lineage leading to *Plantago* (Preston *et al.*, 2011).

The role of *RAD* in *A. majus* is to negatively regulate *DIV* in regions of the flower where *CYC2* genes and *DIV* gene expression spatially overlap. RAD does this by sequestering co-regulators of DIV transcriptional activity in the cytoplasm, thus preventing or reducing DIV activity in the nucleus (Raimundo *et al.*, 2013). In *Antirrhinum*, *RAD* is not expressed in *cyc/dich* double mutant flowers and late expression of *DIV* spreads to all five petals, resulting in radially symmetric (actinomorphic) flowers with all petals having ventral petal identity and shape (Luo *et al.*, 1996, 1999; Galego & Almeida, 2002). Preston *et al.* (2011) previously proposed that the evolution of flower shape in *Plantago* involved loss of the entire floral symmetry gene network (A-clade *CYC*, *RAD* and *DIV*) which resulted in actinomorphic flowers with the default lateral floral organ identity program in place across the whole flower. However, this study demonstrates that a ventral identity program is maintained in *Plantago*. *DIV* orthologs were identified in both *P. lanceolata* and *P. major*, representative species from the two main *Plantago* subgenera (*Psyllium* and *Plantago*; Rønsted *et al.*, 2002), which suggests that the program is probably retained throughout the genus. Thus, the route to actinomorphy in *Plantago* involved loss of only the dorsal identity program, leaving the ventral identity program in place and operational across the whole flower, and in addition acquiring a novel role during stamen and pollen development.

References

Almeida J, Rocheta M, Galego L. 1997. Genetic control of flower shape in *Antirrhinum majus*. *Development* **124**: 1387–1392.

Balk J, Leaver CJ. 2001. The Pet1-CMS mitochondrial mutation in sunflower is associated with premature programmed cell death and cytochrome c release. *Plant Cell* **13**: 1803–1818.

Baxter ELC, Costa MMR, Coen ES. 2007. Diversification and co-option of RAD-like genes in the evolution of floral asymmetry. *Plant Journal* **52**: 105–113.

Bino RJ. 1985. Ultrastructural aspects of cytoplasmic male sterility in *Petunia hybrida*. *Protoplasma* **127**: 230–240.

Boyden GS, Donoghue MJ, Howarth DG. 2012. Duplications and expression of *RADIALIS*-like genes in Dipsacales. *International Jounal of Plant Sciences* **173**: 971–983.

Broholm SK, Tähtiharju S, Laitinen RAE, Albert VA, Teeri TH, Elomaa P. 2008. A TCP domain transcription factor controls flower type specification

along the radial axis of the *Gerbera* (Asteraceae) inflorescence. *Proceedings of the National Academy of Sciences, USA* **105**: 9117–9122.

Busch A, Zachgo S. 2007. Control of corolla monosymmetry in the Brassicaceae *Iberis amara*. *Proceedings of the National Academy of Sciences, USA* **104**: 16714–16719.

Carlsson J, Leino M, Sohlberg J, Sundström JF, Glimelius K. 2008. Mitochondrial regulation of flower development. *Mitochondrion* **8**: 74–86.

Chapman MA, Tang S, Draeger D, Nambeesan S, Shaffer H, Barb JG, Knapp SJ, Burke JM. 2012. Genetic analysis of floral symmetry in Van Gogh's sunflowers reveals independent recruitment of *CYCLOIDEA* genes in the Asteraceae. *PLoS Genetics* **8**: e1002628.

Citerne H, Jabbour F, Nadot S, Damerval C. 2010. The evolution of floral symmetry. *Advances in Botanical Research* **54**: 85–137.

Citerne HL, Pennington RT, Cronk QC. 2006. An apparent reversal in floral symmetry in the legume *Cadia* is a homeotic transformation. *Proceedings of the National Academy of Sciences, USA* **32**: 1217–1220.

Coen ES. 1996. Floral symmetry. *EMBO Journal* **15**: 6777–6788.

Corley SB, Carpenter R, Copsey L, Coen E. 2005. Floral asymmetry involves an interplay between TCP and MYB transcription factors in *Antirrhinum*. *Proceedings of the National Academy of Sciences, USA* **102**: 5068–5073.

Cubas P, Coen E, Zapater JMM. 2001. Ancient asymmetries in the evolution of flowers. *Current Biology* **11**: 1050–1052.

Cubas P, Lauter N, Doebley J, Coen E. 1999a. The TCP domain: a motif found in proteins regulating plant growth and development. *Plant Journal* **18**: 215–222.

Cubas P, Vincent C, Coen E. 1999b. An epigenetic mutation responsible for natural variation in floral symmetry. *Nature* **401**: 157–161.

van Damme JMM, van Delden W. 1982. Gynodioecy in *Plantago lanceolata* L. I. Polymorphism for plasmon type. *Heredity* **49**: 303–318.

De Haan AA, Luyten RMJM, Bakx-Schotman TJMT, van Damme JMM. 1997. The dynamics of gynodioecy in *Plantago lanceolata* L. I. Frequencies of male-steriles and their cytoplasmic male sterility types. *Heredity* **79**: 453–462.

Delph LF, Touzet P, Bailey MF. 2006. Merging theory and mechanism in studies of gynodioecy. *Trends in Ecology and Evolution* **22**: 17–24.

Doyle JA, Endress PK. 2000. Morphological phylogenetic analysis of basal angiosperms: comparison and combination with morphological data. *International Journal of Plant Sciences* **161**: S121–S153.

Endress PK, Doyle JA. 2009. Reconstructing the ancestral angiosperm flower and its initial specializations. *American Jounal of Botany* **96**: 22–66.

Feng X, Zhao Z, Tian Z, Xu S, Luo Y, Cai Z, Wang Y, Yang J, Wang Z, Weng L *et al.* 2006. Control of petal shape and floral zygomorphy in *Lotus japonicus*. *Proceedings of the National Academy of Sciences, USA* **103**: 4970–4975.

Galego L, Almeida J. 2002. Role of *DIVARICATA* in the control of dorsoventral asymmetry in *Antirrhinum* flowers. *Genes & Development* **16**: 880–891.

Grant I, Beversdorf WD, Peterson RL. 1986. A comparative light and electron microscopic study of microspore and tapetal development in male fertile and cytoplasmic male sterile oilseed rape (*Brassica napus*). *Canadian Journal of Botany* **64**: 1055–1068.

Guindon S, Gascuel O. 2003. A simple, fast, and accurate algorithm to estimate large phylogenies by maximum likelihood. *Systematic Biology* **52**: 696–704.

Hileman LC, Kramer EM, Baum DA. 2003. Differential regulation of symmetry genes and the evolution of floral morphologies. *Proceedings of the National Academy of Sciences, USA* **100**: 12814–12819.

Horner HT, Rogers MA. 1974. A comparative light and electron microscopic study of microsporogenesis in male-fertile and cytoplasmic male sterile pepper (*Capsicum annuum*). *Canadian Journal of Botany* **52**: 435–441.

Howarth DG, Donoghue MJ. 2006. Phylogenetic analysis of the "ECE" (CYC/TB1) clade reveals duplications predating the core eudicots. *Proceedings of the National Academy of Sciences, USA* **103**: 9101–9106.

Kapoor S, Kobayashi A, Takatsuji H. 2002. Silencing of the tapetum-specific zinc finger gene *TAZ1* causes premature degeneration of tapetum and pollen abortion in *Petunia*. *Plant Cell* **14**: 2353–2367.

Keane TM, Creevey CJ, Pentony MM, Naughton TJ, McInerney JO. 2006. Assessment of methods for amino acid matrix selection and their use on

empirical data shows that ad hoc assumptions for choice of matrix are not justified. *BMC Evolutionary Biology* **6**: 29.

Kim M, Cui ML, Cubas P, Gillies A, Lee K, Chapman MA, Abbott RJ, Coen ES. 2008. Regulatory genes control a key morphological and ecological trait transferred between species. *Science* **322**: 1116–1119.

Ku S, Yoon H, Suh H, Chung Y. 2003. Male-sterility of thermosensitive genic male-sterile rice is associated with premature programmed cell death of the tapetum. *Planta* **217**: 559–565.

Luo D, Carpenter R, Copsey L, Vincent C, Clark J, Coen E. 1999. Control of organ asymmetry in flowers of *Antirrhinum*. *Cell* **99**: 367–376.

Luo D, Carpenter R, Vincent C, Copsey L, Coen E. 1996. Origin of floral asymmetry in *Antirrhinum*. *Nature* **383**: 794–799.

Martin-Trillo M, Cubas P. 2009. TCP-genes: a family snapshot ten years later. *Trends in Plant Science* **15**: 31–39.

Olmstead RG, dePamphilis CW, Wolfe AD, Young ND, Elisons WJ, Reeves PA. 2001. Disintegration of the Scrophulariaceae. *American Journal of Botany* **88**: 348–361.

Parish RW, Li SF. 2010. Death of a tapetum: a programme of developmental altruism. *Plant Science* **178**: 73–89.

Preston JC, Martinez CC, Hileman LC. 2011. Gradual disintegration of the floral symmetry gene network is implicated in the evolution of a wind-pollination syndrome. *Proceedings of the National Academy of Sciences, USA* **108**: 2343–2348.

Raimundo J, Sobral R, Bailey P, Azevedo H, Galego L, Coen E, Costa MM. 2013. A subcellular tug of war involving three MYB-like proteins underlies a molecular antagonism in *Antirrhinum* flower asymmetry. *Plant Journal* **75**: 527–538.

Reardon W, Fitzpatrick DA, Fares MA, Nugent JM. 2009. Evolution of flower shape in *Plantago lanceolata*. *Plant Molecular Biology* **71**: 241–250.

Reeves PA, Olmstead RG. 1998. Evolution of novel morphological and reproductive traits in a clade containing *Antirrhinum majus* (Scrophulariaceae). *American Journal of Botany* **85**: 1047–1056.

Ronse De Craene LP, Soltis PS, Soltis DE. 2003. Evolution of floral structures in basal angiosperms. *International Journal of Plant Sciences* **164**(Suppl. 5): S329–S363.

Rønsted N, Chase MW, Albach DC, Bello MA. 2002. Phylogenetic relationships within *Plantago* (Plantaginaceae): evidence from nuclear ribosomal ITS and plastid *trnL-F* sequence data. *Botanical Journal of the Linnean Society* **139**: 323–338.

Sargent RD. 2004. Floral symmetry affects speciation rates in angiosperms. *Proceedings of the Royal Society of London, Series B: Biological Sciences* **271**: 603–608.

Shimodaira H. 2002. An approximately unbiased test of phylogenetic tree selection. *Systematic Biology* **51**: 492–508.

Thompson JD, Gibson TJ, Higgins DG. 2002. Multiple sequence alignment using ClustalW and ClustalX. *Current Protocols in Bioinformatics* Chapter 2: Unit 2.3 tree selection. doi: 10.1002/0471250953.bi0203s00 0.

Wang Z, Luo Y, Li X, Wang L, Xu S, Yang J, Weng L, Sato S, Tabata S, Ambrose M *et al.* 2008. Genetic control of floral zygomorphy in pea (*Pisum sativum* L.). *Proceedings of the National Academy of Sciences, USA* **105**: 10414–10419.

Wilson ZA, Morroll SM, Dawson J, Swarup R, Tighe PJ. 2001. The *Arabidopsis MALE STERILITY1* (*MS1*) gene is a transcriptional regulator of male gametogenesis, with homology to the PHD-finger family of transcription factors. *Plant Journal* **28**: 27–39.

Zhang W, Kramer EM, Davis CC. 2010. Floral symmetry genes and the origin and maintenance of zygomorphy in a plant–pollinator mutualism. *Proceedings of the National Academy of Sciences, USA* **107**: 6388–6393.

Zhang W, Steinmann VW, Nikolov L, Kramer EM, Davis C. 2013. Divergent genetic mechanisms underlie reversals to radial floral symmetry from diverse zygomorphic flowered ancestors. *Frontiers in Plant Science* **4**: 302.

Zhou X-R, Wang Y-Z, Smith JF, Chen R. 2008. Altered expression patterns of TCP and MYB genes relating to the floral developmental transition from initial zygomorphy to actinomorphy in *Bournea* (Gesneriaceae). *New Phytologist* **178**: 532–543.

Supporting Information

Additional supporting information may be found in the online version of this article.

Table S1 PCR primers used in this study

Table S2 *DIVARICATA* gene references

Table S3 *RADIALIS* gene references

Please note: Wiley Blackwell are not responsible for the content or functionality of any supporting information supplied by the authors. Any queries (other than missing material) should be directed to the *New Phytologist* Central Office.

About *New Phytologist*

- *New Phytologist* is an electronic (online-only) journal owned by the New Phytologist Trust, a **not-for-profit organization** dedicated to the promotion of plant science, facilitating projects from symposia to free access for our Tansley reviews.

- Regular papers, Letters, Research reviews, Rapid reports and both Modelling/Theory and Methods papers are encouraged. We are committed to rapid processing, from online submission through to publication 'as ready' via *Early View* – our average time to decision is <25 days. There are **no page or colour charges** and a PDF version will be provided for each article.

- The journal is available online at Wiley Online Library. Visit **www.newphytologist.com** to search the articles and register for table of contents email alerts.

- If you have any questions, do get in touch with Central Office (np-centraloffice@lancaster.ac.uk) or, if it is more convenient, our USA Office (np-usaoffice@ornl.gov)

- For submission instructions, subscription and all the latest information visit **www.newphytologist.com**